

Parton distribution functions from Lattice QCD

Savvas Zafeiropoulos

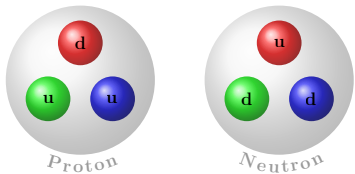
CPT, Marseille

IGFAE virtual seminar

Santiago de Compostela

In collaboration with J. Karpie (Columbia), K. Orginos (College of William & Mary and JLAB), A. Radyushkin (ODU and JLAB)
D. Richards (JLAB), R. Sufian (JLAB) and A. Rothkopf (Stavanger U)

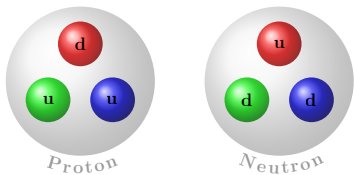
Defining Parton Distribution Functions (PDFs)



- Parton is the name proposed by R. Feynman in 1969 as a generic description of the particles that constitute the nucleons.

- A model assuming that the nucleon is made out of three valence quarks in a bag is way too simple!
- It can not reproduce the experimental results for scattering processes with inelastic scattering of electrons off protons.
- Actually hadrons are relativistic many body systems where valence quarks are "embedded" in a sea of virtual $q - \bar{q}$ pairs created by the gluons...
- The nucleon structure is experimentally very intensively investigated, but can in principle be accessed also with theoretical calculations

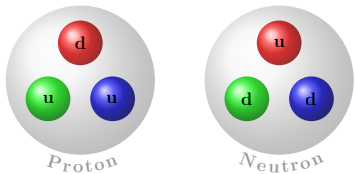
Defining Parton Distribution Functions (PDFs)



- Parton is the name proposed by R. Feynman in 1969 as a generic description of the particles that constitute the nucleons.

- A model assuming that the nucleon is made out of three valence quarks in a bag is way too simple!
- It can not reproduce the experimental results for scattering processes with inelastic scattering of electrons off protons.
- Actually hadrons are relativistic many body systems where valence quarks are "embedded" in a sea of virtual $q - \bar{q}$ pairs created by the gluons...
- The nucleon structure is experimentally very intensively investigated, but can in principle be accessed also with theoretical calculations

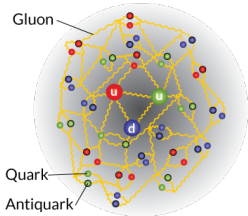
Defining Parton Distribution Functions (PDFs)



- Parton is the name proposed by R. Feynman in 1969 as a generic description of the particles that constitute the nucleons.

- A model assuming that the nucleon is made out of three valence quarks in a bag is way too simple!
- It can not reproduce the experimental results for scattering processes with inelastic scattering of electrons off protons.
- Actually hadrons are relativistic many body systems where valence quarks are "embedded" in a sea of virtual $q - \bar{q}$ pairs created by the gluons...
- The nucleon structure is experimentally very intensively investigated, but can in principle be accessed also with theoretical calculations

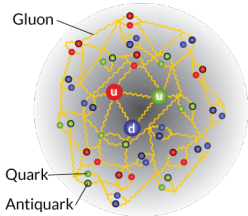
Defining Parton Distribution Functions (PDFs)



- Parton is the name proposed by R. Feynman in 1969 as a generic description of the particles that constitute the nucleons.

- A model assuming that the nucleon is made out of three valence quarks in a bag is way too simple!
- It can not reproduce the experimental results for scattering processes with inelastic scattering of electrons off protons.
- Actually hadrons are relativistic many body systems where valence quarks are "embedded" in a sea of virtual $q - \bar{q}$ pairs created by the gluons...
- The nucleon structure is experimentally very intensively investigated, but can in principle be accessed also with theoretical calculations

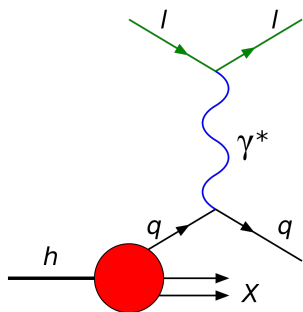
Defining Parton Distribution Functions (PDFs)



- Parton is the name proposed by R. Feynman in 1969 as a generic description of the particles that constitute the nucleons.

- A model assuming that the nucleon is made out of three valence quarks in a bag is way too simple!
- It can not reproduce the experimental results for scattering processes with inelastic scattering of electrons off protons.
- Actually hadrons are relativistic many body systems where valence quarks are "embedded" in a sea of virtual $q - \bar{q}$ pairs created by the gluons...
- The nucleon structure is experimentally very intensively investigated, but can in principle be accessed also with theoretical calculations

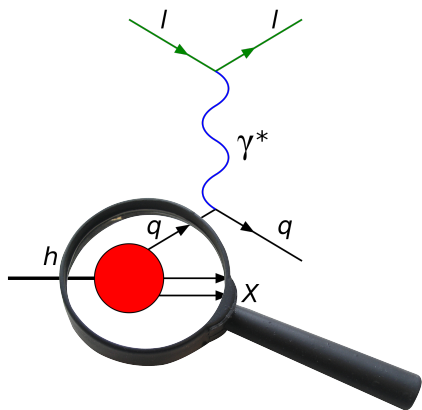
Defining Parton Distribution Functions (PDFs)



Deep Inelastic Scattering (DIS)

- In DIS processes leptons act as a probe transferring “four-momentum” q to the nucleon to resolve the partonic structure.
- Resolving power of the probe given by $1/q$. Resolution increases with q . With $q = 100$ GeV, the resolution is 0.02 fm.
- Friedman, Kendall and Taylor were awarded the Nobel prize in 1990 for their pioneering experiments at SLAC in 1966 which showed the first evidence of partonic structure of the nucleon.

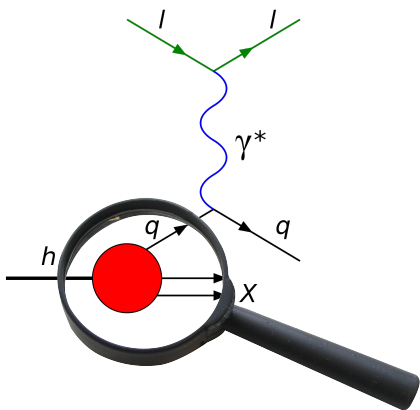
Defining Parton Distribution Functions (PDFs)



Deep Inelastic Scattering (DIS)

- In DIS processes leptons act as a probe transferring “four-momentum” q to the nucleon to resolve the partonic structure.
- Resolving power of the probe given by $1/q$. Resolution increases with q . With $q = 100$ GeV, the resolution is 0.02 fm.
- Friedman, Kendall and Taylor were awarded the Nobel prize in 1990 for their pioneering experiments at SLAC in 1966 which showed the first evidence of partonic structure of the nucleon.

Defining Parton Distribution Functions (PDFs)



Deep Inelastic Scattering (DIS)

- In DIS processes leptons act as a probe transferring “four-momentum” q to the nucleon to resolve the partonic structure.
- Resolving power of the probe given by $1/q$. Resolution increases with q . With $q = 100$ GeV, the resolution is 0.02 fm.
- Friedman, Kendall and Taylor were awarded the Nobel prize in 1990 for their pioneering experiments at SLAC in 1966 which showed the first evidence of partonic structure of the nucleon.

Defining Parton Distribution Functions (PDFs)

- The target in the DIS experiments can be seen as a stream of partons carrying a fraction x of the longitudinal momentum.
- The momentum distribution functions of partons within the proton are called Parton Distribution Functions (PDFs).
- They represent probability densities to find a parton carrying a fraction x of the nucleon momentum at squared energy scale $Q^2 = -q^2$.

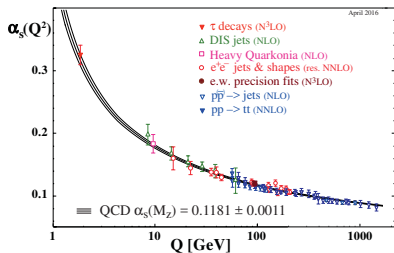
Defining Parton Distribution Functions (PDFs)

- The target in the DIS experiments can be seen as a stream of partons carrying a fraction x of the longitudinal momentum.
- The momentum distribution functions of partons within the proton are called Parton Distribution Functions (PDFs).
- They represent probability densities to find a parton carrying a fraction x of the nucleon momentum at squared energy scale $Q^2 = -q^2$.

Defining Parton Distribution Functions (PDFs)

- The target in the DIS experiments can be seen as a stream of partons carrying a fraction x of the longitudinal momentum.
- The momentum distribution functions of partons within the proton are called Parton Distribution Functions (PDFs).
- They represent probability densities to find a parton carrying a fraction x of the nucleon momentum at squared energy scale $Q^2 = -q^2$.

Defining Parton Distribution Functions (PDFs)

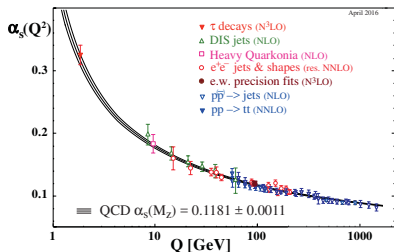


Scale-dependent coupling constant

- A key property of QCD is asymptotic freedom.
- Interactions between partons become arbitrarily weak at higher and higher energies or shorter and shorter distances.

- Perturbation theory can make predictions about the rate of change (evolution) of PDFs when the energy scale Q^2 changes.
- The QCD evolution equations were discovered by Dokshitzer (1977), Gribov, Lipatov (1972), Altarelli and Parisi (1977) and are called the DGLAP equations.
- The x dependence of the PDFs can not be predicted by perturbation theory.

Defining Parton Distribution Functions (PDFs)

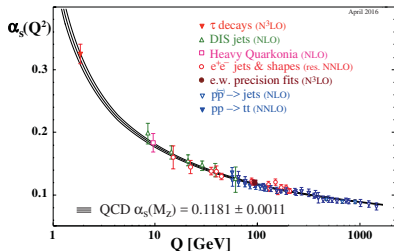


Scale-dependent coupling constant

- A key property of QCD is asymptotic freedom.
- Interactions between partons become arbitrarily weak at higher and higher energies or shorter and shorter distances.

- Perturbation theory can make predictions about the rate of change (evolution) of PDFs when the energy scale Q^2 changes.
- The QCD evolution equations were discovered by Dokshitzer (1977), Gribov, Lipatov (1972), Altarelli and Parisi (1977) and are called the DGLAP equations.
- The x dependence of the PDFs can not be predicted by perturbation theory.

Defining Parton Distribution Functions (PDFs)

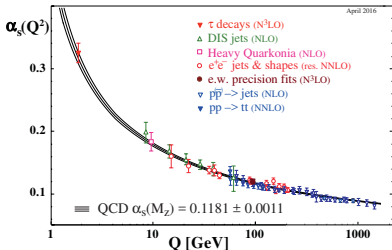


Scale-dependent coupling constant

- A key property of QCD is asymptotic freedom.
- Interactions between partons become arbitrarily weak at higher and higher energies or shorter and shorter distances.

- Perturbation theory can make predictions about the rate of change (evolution) of PDFs when the energy scale Q^2 changes.
- The QCD evolution equations were discovered by Dokshitzer (1977), Gribov, Lipatov (1972), Altarelli and Parisi (1977) and are called the DGLAP equations.
- The x dependence of the PDFs can not be predicted by perturbation theory.

Defining Parton Distribution Functions (PDFs)

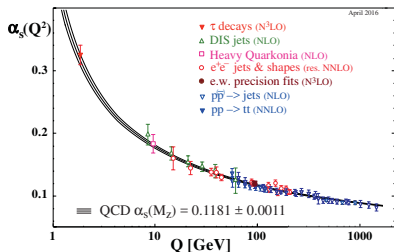


Scale-dependent coupling constant

- A key property of QCD is asymptotic freedom.
- Interactions between partons become arbitrarily weak at higher and higher energies or shorter and shorter distances.

- Perturbation theory can make predictions about the rate of change (evolution) of PDFs when the energy scale Q^2 changes.
- The QCD evolution equations were discovered by Dokshitzer (1977), Gribov, Lipatov (1972), Altarelli and Parisi (1977) and are called the DGLAP equations.
- The x dependence of the PDFs can not be predicted by perturbation theory.

Defining Parton Distribution Functions (PDFs)



Scale-dependent coupling constant

- A key property of QCD is asymptotic freedom.
- Interactions between partons become arbitrarily weak at higher and higher energies or shorter and shorter distances.

- Perturbation theory can make predictions about the rate of change (evolution) of PDFs when the energy scale Q^2 changes.
- The QCD evolution equations were discovered by Dokshitzer (1977), Gribov, Lipatov (1972), Altarelli and Parisi (1977) and are called the DGLAP equations.
- The x dependence of the PDFs can not be predicted by perturbation theory.

PDFs are of paramount importance because...

- The uncertainties in PDFs are the **dominant theoretical uncertainties** in Higgs couplings, α_s and the mass of the W boson

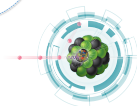
- Beyond the LHC, PDFs play an important role, for instance in astroparticle physics, such as for the accurate predictions for signal and background events at ultra-high energy neutrino telescopes (ANITA, IceCube, Pierre Auger Observatory)



Future Circular Collider
Circumference: 80-100 km
Energy: 100 TeV (pp)
>350 GeV (e⁺e⁻)

Large Hadron Collider
Circumference: 27 km
Energy: 14 TeV (pp)
209 GeV (e⁺e⁻)

Tevatron (closed)
Circumference: 6.2 km
Energy: 2 TeV

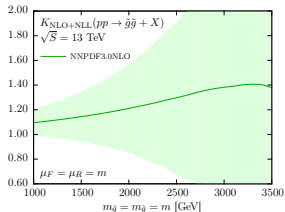
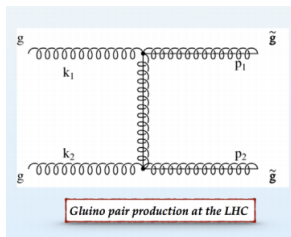


- PDFs will keep playing an important role for any future high energy collider involving hadrons in the initial state. Therefore improving our understanding of PDFs also strengthens the physics potential of such future colliders

 Gao, Harland-Lang, Rojo (2018)

PDF uncertainties and BSM Physics

The uncertainty on the PDFs is rapidly becoming one of the limiting factors in searches for new physics.



The relative size of the NLL corrections for gluino pair production was computed. The error in the relative size of the NLL corrections grows very quickly as the gluino mass is increased, mostly as a consequence of the large PDF errors at large values of x . [Beenakker et al. \(2016\)](#)

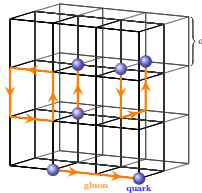
From DIS to PDFs via factorization

- The measurement of PDFs is made possible due to factorization theorems
- Intuitively, factorization theorems tell us that the same universal non-perturbative objects (the PDFs), representing long distance physics, can be combined with many short-distance calculations in QCD to give the cross-sections of various processes

$$\sigma = f \otimes H$$

- ▶ f are the PDFs, H is the hard perturbative part and \otimes is convolution.
- ▶ PDFs truly characterize the hadronic target
- ▶ PDFs are essentially non-perturbative

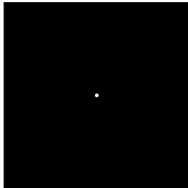
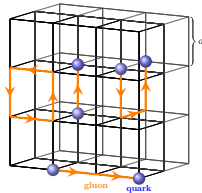
Lattice?



- The natural ab-initio method to study QCD non-perturbatively is on the lattice. But ...
- PDFs are defined as an expectation value of a bilocal operator evaluated along a light-like line.
- Clearly, we can not evaluate this on a Euclidean set-up.



Lattice?



- The natural ab-initio method to study QCD non-perturbatively is on the lattice. But ...
- PDFs are defined as an expectation value of a bilocal operator evaluated along a light-like line.
- Clearly, we can not evaluate this on a Euclidean set-up.

Lattice traditionally & global PDF fits

Light cone PDF

$$\hookrightarrow q(x) = \frac{1}{4\pi} \int_{-\infty}^{\infty} d\omega^- e^{-ixP^+\omega^-} \langle P | \bar{\psi}(\omega^-) W(\omega^-, 0) \gamma^+ \psi(0) | P \rangle$$

$$\text{where } W(\omega^-, 0) = \mathcal{P} e^{-ig_0 \int_0^{\omega^-} dy^- A^+(y^-)}$$

Lattice traditionally & global PDF fits

Light cone PDF

$$\hookrightarrow q(x) = \frac{1}{4\pi} \int_{-\infty}^{\infty} d\omega^- e^{-ixP^+\omega^-} \langle P | \bar{\psi}(\omega^-) W(\omega^-, 0) \gamma^+ \psi(0) | P \rangle$$

Mellin moments $\langle x^k \rangle_q = \int_{-1}^1 dx x^k q(x)$ related to local matrix elements of twist-2 operators

$$\langle P | \bar{\psi}(0) \gamma^{\{\mu_1} D^{\mu_2} \dots D^{\mu_k\}} \psi(0) | P \rangle = 2 \langle x^k \rangle_q (P^{\mu_1} \dots P^{\mu_k} - \text{traces})$$

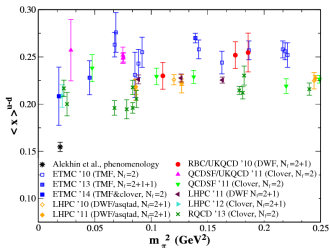
Lattice traditionally & global PDF fits

- Not an issue if every moment were accessible because a probability distribution is completely determined once all its moments are known.
 - These studies are limited to the first few (three) moments due to
 - ▶ Bad signal to noise ratio
 - ▶ Power-divergent mixing on the lattice (discretized space-time does not possess the full rotational symmetry of the continuum).
-

Lattice traditionally & global PDF fits

Mellin moments

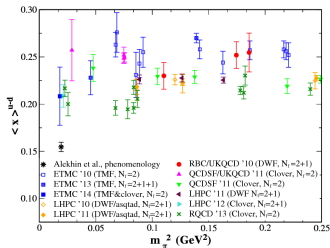
 Constantinou (2015)



Lattice traditionally & global PDF fits

Mellin moments

Constantinou (2015)



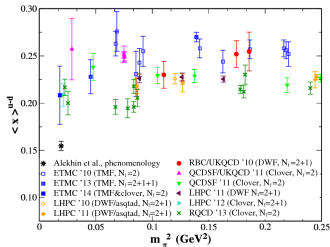
Global fits

- Usual determination of PDFs is performed by fitting experimental data from several hard scattering cross sections (l-p and p-p collisions)
- Combining the most PDF-sensitive data and the highest precision QCD and EW calculations (always assuming that SM holds) and employing a statistically robust fitting methodology
- Can achieve high precision for the cases that data are abundant

Lattice traditionally & global PDF fits

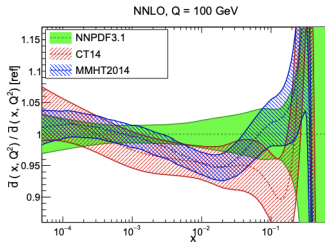
Mellin moments

Constantinou (2015)



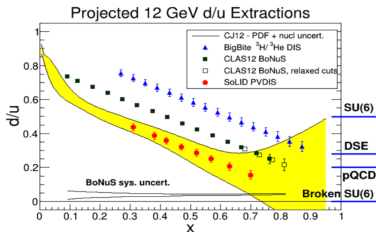
Global fits

Lin et al. (2018)



Large- x discrepancies for the nucleon and the pion

The nucleon



- JLab 12-GeV measurements of the ratio of the PDFs for the d and u quarks at large momentum fraction x
- In yellow the projected uncertainty in measurements under several theoretical assumptions

The pion

Model/theory	large x
QCD parton model	$(1-x)^2$
pQCD	$(1-x)^{2+\gamma}$
Light-front holographic QCD	$(1-x)^0$
Nambu-Jona-Lasino/duality	$(1-x)^1$

- \bar{u} quark distribution of π^- extracted @FNAL E615
- Large- x of pion PDF is the goal @JLab-C12-15-006, @COMPASS-CERN. Large- x of kaon PDF is the goal @JLab-C12-15-006A

An ab-initio non-perturbative QCD calculation is timely and imperative!

PDFs from the lattice: Pseudo-PDFs Formalism

Starting point: the equal time hadronic matrix element with the quark and anti-quark fields separated by a finite distance [Radyushkin \(2017\)](#)

$$\mathcal{M}^\alpha(z, p) \equiv \langle p | \bar{\psi}(0) \gamma^\alpha \hat{E}(0, z; A) \tau_3 \psi(z) | p \rangle$$

$z = (0, 0, 0, z_3)$
 $p = (p^0, 0, 0, p)$
 $\alpha = 0$

Lorentz inv. \rightarrow

$$\mathcal{M}^\alpha(z, p) = 2p^\alpha \underbrace{\mathcal{M}_p(-z p, -z^2)}_{\text{Leading twist}} + z^\alpha \underbrace{\mathcal{M}_z(-z p, -z^2)}_{\text{Higher twist}}$$

- The Lorentz invariant quantity $\nu = -(z p)$, is the "loffe time"
- loffe time PDFs $\mathcal{M}(\nu, z_3^2)$ defined at a scale $\mu^2 = 4e^{-2\gamma_E}/z_3^2$ (at leading log level) are the Fourier transform of regular PDFs $f(x, \mu^2)$ [Balitsky, Braun \(1988\)](#), [Braun et al. \(1995\)](#)

$$\mathcal{M}(\nu, z_3^2) = \int_{-1}^1 dx f(x, 1/z_3^2) e^{i x \nu}$$

Lattice QCD requirements

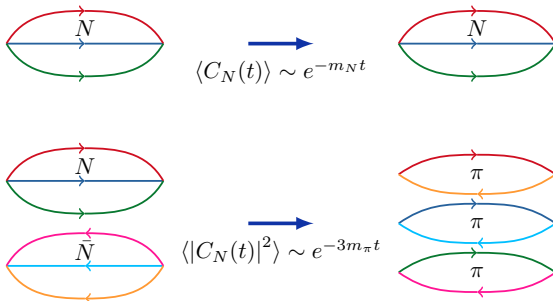
- Largest momentum on the lattice $aP_{max} = \pi/2 \propto \mathcal{O}(1)$
- $a = 0.1\text{fm} \rightarrow P_{max} = 10\Lambda$ where $\Lambda = 300 \text{ MeV}$
- $a = 0.05\text{fm} \rightarrow P_{max} = 20\Lambda$

Large momentum provides a wide coverage of the loffe time ν

$P_{max} = 3 \text{ GeV}$ easily achievable with moderate values of the lattice spacing but still demanding due to statistical noise

$P_{max} = 6 \text{ GeV}$ exponentially harder requiring very fine values of the lattice spacing

Signal to Noise



Statistical accuracy drops exponentially with increasing momentum P


$$\text{StN}(O) = \frac{\langle O \rangle}{\sqrt{\text{var}(O)}} \propto e^{-[E_N(P) - 3/2m_\pi]t}$$

G. Parisi (1984) P. Lepage (1989)

Obtaining the Ioffe time PDF

$$z_3 \rightarrow 0 \Rightarrow \mathcal{M}_p(\nu, z_3^2) = \mathcal{M}(\nu, z_3^2) + \mathcal{O}(z_3^2)$$

But.... large $\mathcal{O}(z_3^2)$ corrections **prohibit** the extraction.

Conservation of the vector current implies $\mathcal{M}_p(0, z_3^2) = 1 + \mathcal{O}(z_3^2)$, but in a **ratio** z_3^2 corrections (related to the transverse structure of the hadron) might cancel  [Radyushkin \(2017\)](#)

$$\mathfrak{M}(\nu, z_3^2) \equiv \frac{\mathcal{M}_p(\nu, z_3^2)}{\mathcal{M}_p(0, z_3^2)}$$

- Much **smaller** $\mathcal{O}(z_3^2)$ corrections and therefore this ratio could be used to extract the Ioffe time PDFs
- All UV singularities are **exactly cancelled** and when computed in lattice QCD it can be extrapolated to the continuum limit at fixed ν and z^2 .

Numerical implementation

First case study in an unphysical setup [Karpie, Orginos, Radyushkin SZ, Phys.Rev. D96 \(2017\) no.9, 094503](#)

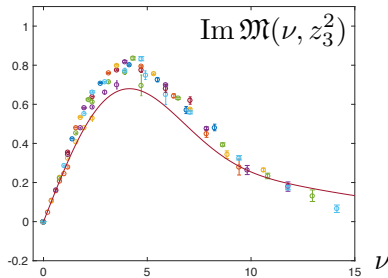
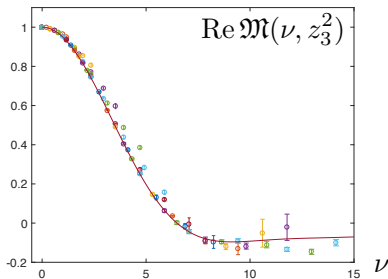
- Quenched approximation
- $32^3 \times 64$ lattices with $a = 0.093\text{fm}$.
- $m_\pi = 601\text{MeV}$ and $m_N = 1411\text{MeV}$

Now employing dynamical ensembles

$a(\text{fm})$	$M_\pi(\text{MeV})$	β	$L^3 \times T$
0.127(2)	415	6.1	$24^3 \times 64$
0.127(2)	415	6.1	$32^3 \times 96$
0.094(1)	390	6.3	$32^3 \times 64$
0.094(1)	280	6.3	$32^3 \times 64$
0.094(1)	172	6.3	$64^3 \times 128$

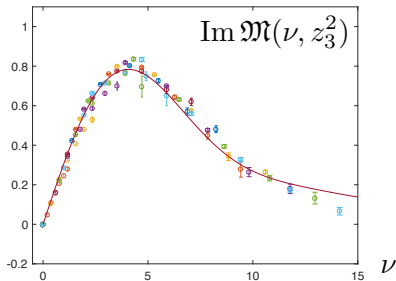
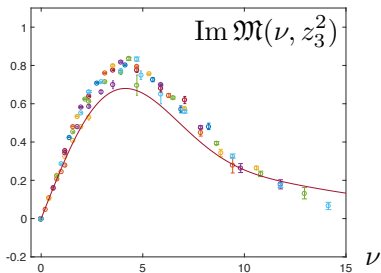
Table: Parameters for the lattices generated by the JLab/W&M collaboration using 2+1 flavors of clover Wilson fermions and a tree-level tadpole-improved Symanzik gauge action. The lattice spacings, a , are estimated using the Wilson flow scale w_0 . Stout smearing implemented in the fermion action makes the tadpole corrected tree-level clover coefficient c_{SW} used, to be very close to the value determined non-pertubatively with the Schrödinger functional method

Results for the Re and Im parts of $\mathfrak{M}(\nu, z_3^2)$



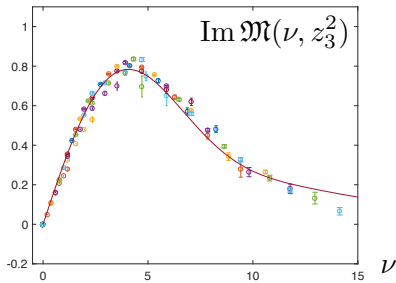
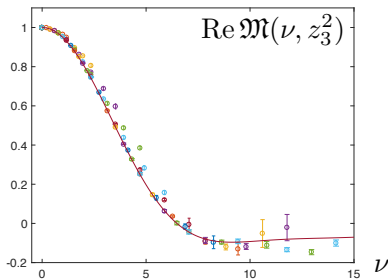
- Curves represent Re and Im Fourier transforms of $q_\nu(x) = \frac{315}{32} \sqrt{x}(1-x)^3$.
- Considering CP even and odd combinations
 - ▶ even: $q_-(x) = f(x) + f(-x) = q(x) - \bar{q}(x) = q_\nu(x)$
 - ▶ odd: $q_+(x) = f(x) - f(-x) = q(x) + \bar{q}(x) = q_\nu(x) + 2\bar{q}(x)$

Results for the Im part of $\mathfrak{M}(\nu, z_3^2)$



- Curves represent the Im Fourier transforms of $q_v(x) = q(x) - \bar{q}(x)$ and $q_+(x) = q(x) + \bar{q}(x) = q_v(x) + 2\bar{q}(x)$ respectively.
- The agreement with the data is strongly improved if we use a non-vanishing antiquark contribution, namely $\bar{q}(x) = \bar{u}(x) + \bar{d}(x) = 0.07[20x(1-x)^3]$.

Results for the Re and Im parts of $\mathfrak{M}(\nu, z_3^2)$



- Data as function of the loffe time. A **residual** z_3 -dependence can be seen.
- This is more visible when, for a **particular** ν we have several data points corresponding to **different values of** z_3 .
- Different values of z_3^2 for the same ν correspond to the loffe time distribution at different scales.

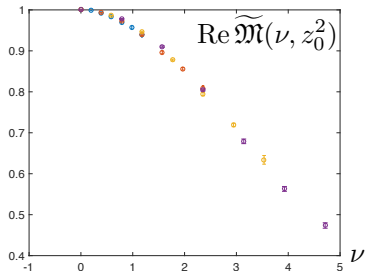
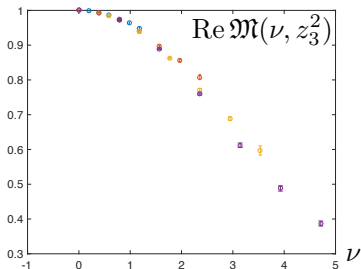
Residual z_3 -dependence

- Is the residual scatter in the data points **consistent with evolution**? By solving the evolution equation at LO, the Ioffe time PDF at z'_3 is related to the one at z_3 by

$$\mathfrak{M}(\nu, z'_3{}^2) = \mathfrak{M}(\nu, z_3^2) - \frac{2}{3} \frac{\alpha_s}{\pi} \ln(z'_3{}^2/z_3^2) \int_0^1 du B(u) \mathfrak{M}(u\nu, z_3^2)$$

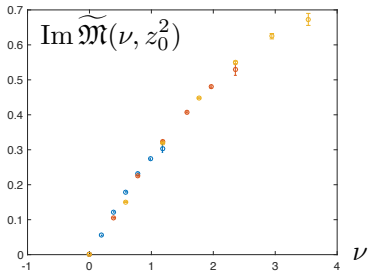
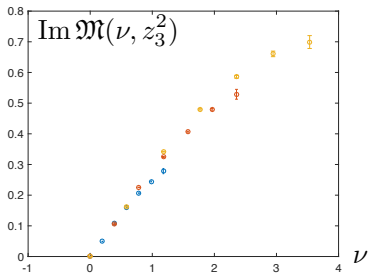
- Only applicable at small z_3

Before and after evolution



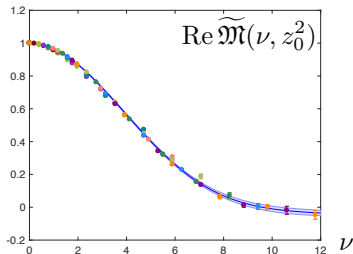
The ratio $\mathfrak{M}(\nu, z_3^2)$ for $z_3/a = 1, 2, 3,$ and 4 . **LHS:** Data before evolution. **RHS:** Data after evolution. The reduction in scatter indicates that evolution collapses all data to the same universal curve.

Before and after evolution



The ratio $\mathfrak{M}(\nu, z_3^2)$ for $z_3/a = 1, 2, 3, \text{ and } 4$. **LHS:** Data before evolution. **RHS:** Data after evolution. The reduction in scatter indicates that evolution collapses all data to the same universal curve.

Comparison to global fits



- Evolved points fitted with cosine FT of

$$q_v(x) = N(a, b) x^a (1 - x)^b$$

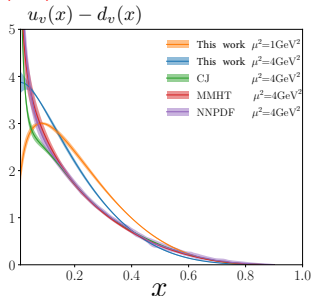
$$a = 0.36(6), \quad b = 3.95(22)$$

 Karpie, Orginos, Radyushkin, S.Z. (2017)

- Evolved data can be exploited to build

$$u_v(x) - d_v(x)$$

- Results compared with predictions from global fits

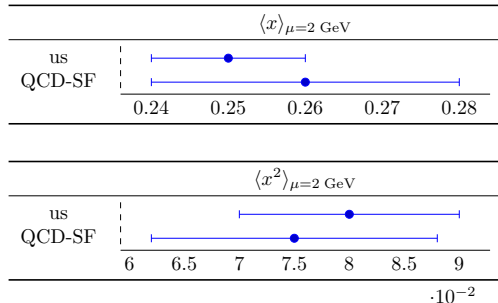


Sanity checks vs other lattice results

- Extract lowest PDF moments from our data [Karpie, Orginos, S.Z., JHEP 1811 \(2018\)](#) and compare with the lattice literature [QCD-SF collaboration \(1996\)](#)
- \overline{MS} moments up to $\mathcal{O}(\alpha_s^2, z^2)$ directly from the reduced function $\mathfrak{M}(\nu, z^2)$

$$a_{n+1}(\mu) = (-i)^n \frac{1}{c_n(z^2 \mu^2)} \left. \frac{\partial^n \mathfrak{M}(\nu, z^2)}{\partial \nu^n} \right|_{\nu=0} + \mathcal{O}(z^2, \alpha_s^2)$$

- Our method avoids mixing and allows the extraction of any moment



The pertinent systematics in PDF extraction


- Parton distribution functions or distribution amplitudes may be defined in lattice QCD by inverting the quasi-Fourier transform of a certain class of hadronic position-space matrix elements
- One example are the Ioffe-time PDFs, \mathfrak{M}_R , related to the physical PDF $q_v(x, \mu^2)$ via the integral relation

$$\mathfrak{M}_R(\nu, \mu^2) \equiv \int_0^1 dx \cos(\nu x) q_v(x, \mu^2)$$

The pertinent systematics in PDF extraction

- Parton distribution functions or distribution amplitudes may be defined in lattice QCD by inverting the quasi-Fourier transform of a certain class of hadronic position-space matrix elements
- One example are the Ioffe-time PDFs, \mathfrak{M}_R , related to the physical PDF $q_v(x, \mu^2)$ via the integral relation

**Only a handful
of lattice data**


$$\mathfrak{M}_R(\nu, \mu^2) \equiv \int_0^1 dx \cos(\nu x) q_v(x, \mu^2)$$

The pertinent systematics in PDF extraction

- Parton distribution functions or distribution amplitudes may be defined in lattice QCD by inverting the quasi-Fourier transform of a certain class of hadronic position-space matrix elements
- One example are the Ioffe-time PDFs, \mathfrak{M}_R , related to the physical PDF $q_v(x, \mu^2)$ via the integral relation

Only a handful
of lattice data

$$\mathfrak{M}_R(\nu, \mu^2) \equiv \int_0^1 dx \cos(\nu x) q_v(x, \mu^2)$$

Cosine not orthogonal in $[0, 1]$

The pertinent systematics in PDF extraction

- Parton distribution functions or distribution amplitudes may be defined in lattice QCD by inverting the quasi-Fourier transform of a certain class of hadronic position-space matrix elements
- One example are the Ioffe-time PDFs, \mathfrak{M}_R , related to the physical PDF $q_v(x, \mu^2)$ via the integral relation

Only a handful
of lattice data

$$\mathfrak{M}_R(\nu, \mu^2) \equiv \int_0^1 dx \cos(\nu x) q_v(x, \mu^2)$$

Cosine not orthogonal in $[0, 1]$

- The task at hand is then to **reconstruct the PDF $q_v(x, \mu^2)$ given a limited set of simulated data** for $\mathfrak{M}_R(\nu, \mu^2)$.
- The extraction is highly ill-posed, so one has to resort to regularization strategies in order to find a way to reliably estimate the PDF from the data at hand

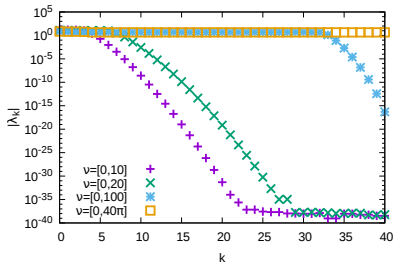
 Karpie, Orginos, Rothkopf, S.Z. JHEP 1904 (2019) 057

Naive Reconstruction

- Discretize the integral, employing the trapezoid rule

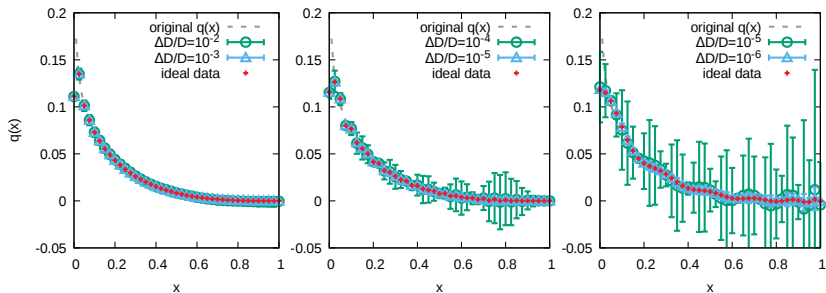
$$\mathfrak{M}_R(\nu) = \frac{1}{2} \cos(\nu x_0) q_\nu(x_0) + \sum_{k=1}^{N_x-1} \delta x \cos(\nu x_k) q_\nu(x_k) + \frac{1}{2} \cos(\nu x_{N_x}) q_\nu(x_{N_x})$$

- Casting our problem in a matrix equation $\mathfrak{m} = \mathfrak{C} \cdot \mathfrak{q}$,
- The conditioning of the problem is easily elucidated by considering the eigenvalues of the matrix \mathfrak{C} .



 Karpie, Orginos, Rothkopf, S.Z. - arXiv:1901.05408 - JHEP 1904 (2019) 057

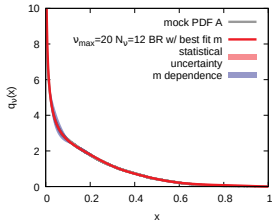
Naive Reconstruction



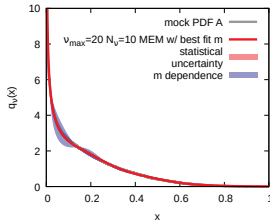
Results for the direct inversion for different discretization intervals
(left $\nu = [0, 40\pi]$, center $\nu = [0, 100]$, right $\nu = [0, 20]$).

Advanced PDF Reconstructions

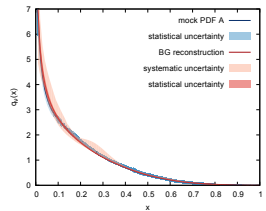
Bayesian Reconstruction



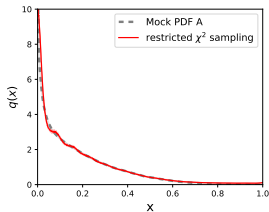
Max. Entropy Method



Backus-Gilbert algorithm

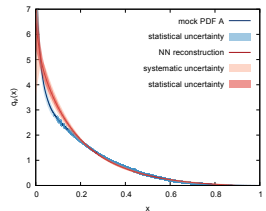


HMC χ^2 evaluation



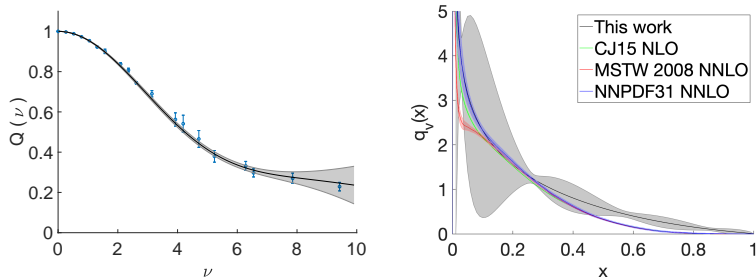
Capitalize of the good scanning in loffe time and use advanced reconstruction methods to extract the maximum amount of information also for the small- x region.

Neural Network



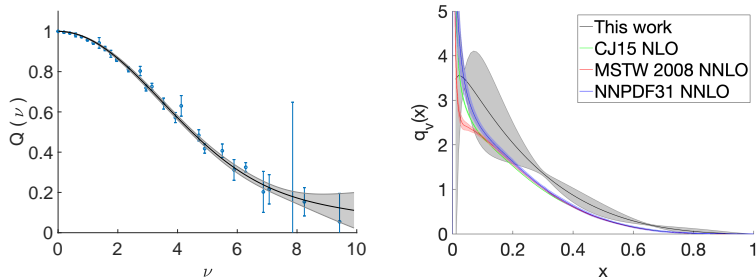
 Karpie, Orginos, Rothkopf, S.Z. JHEP 1904 (2019) 057

New results with $N_f = 2 + 1$ fermions for the nucleon



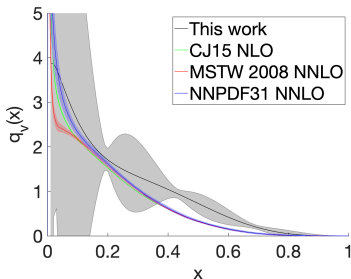
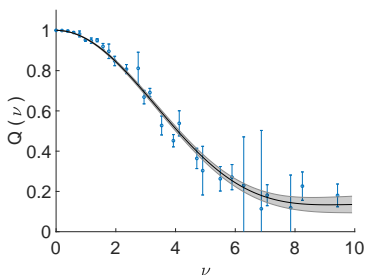
The nucleon valence distribution obtained from the ensemble $a127m415$ fit to the form used by the JAM collaboration. The $\chi^2/\text{d.o.f.}$ for the fit with all the data is 2.5(1.5). The uncertainty band is obtained from the fits to the Jackknife samples of the data.

New results with $N_f = 2 + 1$ fermions for the nucleon



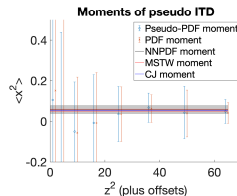
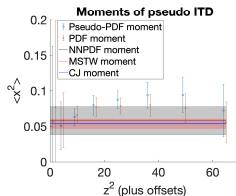
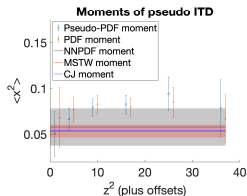
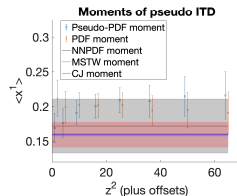
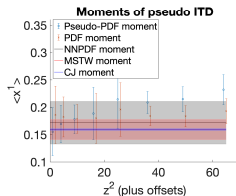
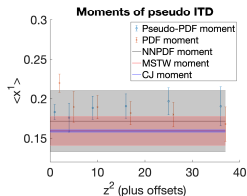
The nucleon valence distribution obtained from the ensemble $a_{127m415L}$ fit to the form used by the JAM collaboration. The $\chi^2/\text{d.o.f.}$ for the fit with all the data is 2.1(6). The uncertainty band is obtained from the fits to the Jackknife samples of the data.

New results with $N_f = 2 + 1$ dynamical fermions

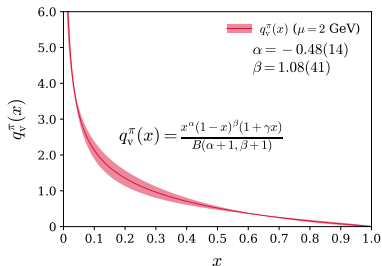
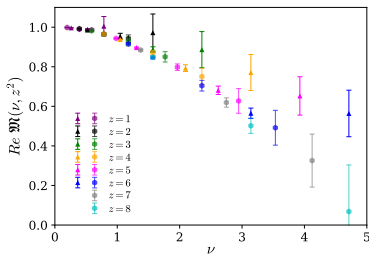


The nucleon valence distribution obtained from the ensemble $a094m390$ fit to the form used by the JAM collaboration. The $\chi^2/\text{d.o.f.}$ for the fit with all the data is 2.0(5). The uncertainty band is obtained from the fits to the Jackknife samples of the data.

New results with $N_f = 2 + 1$ fermions for the nucleon

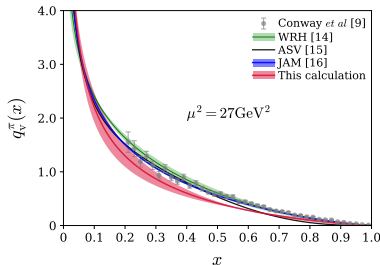
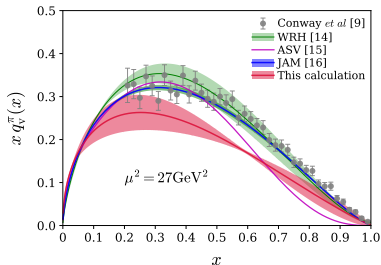


Results with $N_f = 2 + 1$ fermions for the pion



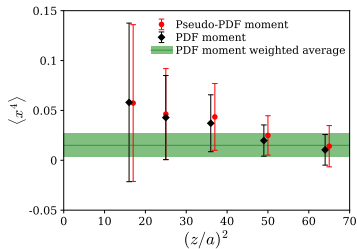
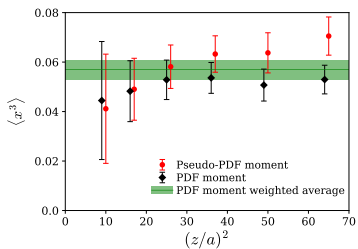
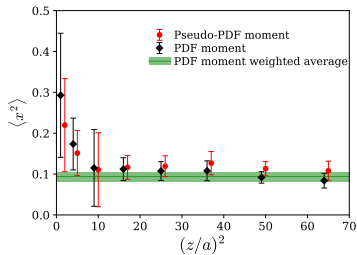
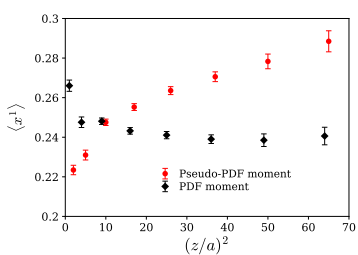
Reduced pseudo-ITD obtained from ensembles $a127m415$ and $a127m415L$ after 1-loop perturbative matching at $\mu = 2$ GeV. The circle (\circ) symbols indicate the reduced pseudo-ITD matrix elements M^0 extracted from the $a127m415$ ensemble and the diamond (\diamond) symbols denote those for the $a127m415L$ ensemble. The red band is obtained from a simultaneous fit to the matched ITDs on these two ensembles in the limit of infinite volume (LHS). The pion valence distribution (RHS).

Results with $N_f = 2 + 1$ flavors for the pion



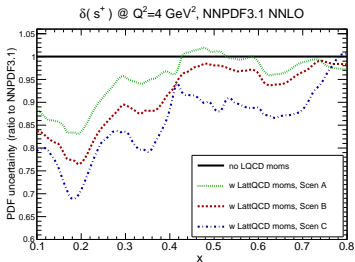
(LHS) Comparison of the pion $xq_V^\pi(x)$ -distribution with the LO extraction from DY data (gray data points), NLO fits (green, maroon, and blue). This lattice QCD calculation of $q_V^\pi(x)$ is evolved from an initial scale $\mu_0^2 = 4\text{ GeV}^2$ at NLO. All the results are evolved to an evolution scale of $\mu^2 = 27\text{ GeV}^2$. Similar comparison of the pion $q_V^\pi(x)$ -distribution (RHS).

Results with $N_f = 2 + 1$ flavors for the pion

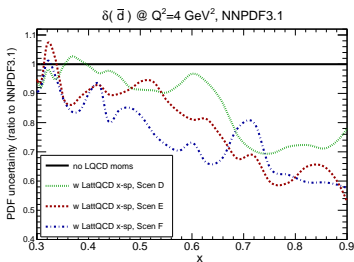


Lattice impact in the precision of global fits

s^+ quark PDFs, percentage PDF uncertainty



\bar{d} quark PDFs, percentage PDF uncertainty



- The comparison is with the results of including lattice-QCD pseudo-data for moments of PDFs (left) and info from lattice-QCD pseudo-data on x-space PDFs (right). [Lin et al. \(2018\)](#)

Conclusions and outlook

- PDFs are needed as theoretical inputs to all hadron scattering experiments and in some cases are the largest theory uncertainty.
- The lattice community is by now able to provide ab-initio determinations of PDFs without theoretical obstructions.
- The interplay between lattice QCD and global fits is very important
- Also important in the search of New Physics [Gao, Harland-Lang, Rojo \(2018\)](#)
- What next? Polarized, Transversity, gluon PDFs and GPDs eventually
- **Many thanks for your attention!!!**

Formalism

- The quasi-PDF $Q(x, p^2)$ is related to $\mathcal{M}_p(\nu, z_3^2)$ by

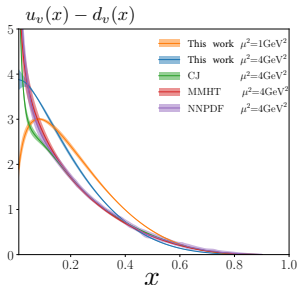
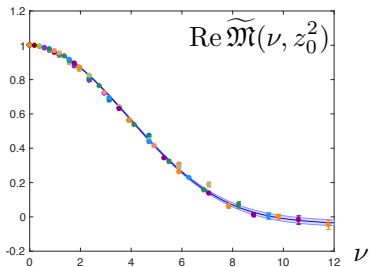
$$Q(x, p^2) = \frac{1}{2\pi} \int_{-\infty}^{\infty} d\nu e^{-ix\nu} \mathcal{M}_p(\nu, [\nu/p]^2)$$

Quasi PDF mixes invariant scales until p_z is effectively large enough

- While the pseudo-PDF has fixed invariant scale dependence

$$P(x, z_0^2) = \frac{1}{2\pi} \int_{-\infty}^{\infty} d\nu e^{-ix\nu} \mathcal{M}_p(\nu, z_0^2)$$

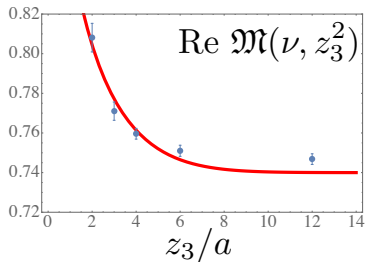
Comparison to global fits



LHS: Data points for $\text{Re } \widetilde{\mathcal{M}}(\nu, z_3^2)$ with $z_3 \leq 10a$ evolved to $z_3 = 2a$. By fitting these evolved points with a cosine FT of $q_v(x) = N(a, b)x^a(1-x)^b$ we obtain $a = 0.36(6)$ and $b = 3.95(22)$ (statistical errors). RHS: Curve for $u_v(x) - d_v(x)$ built from the evolved data shown in the left panel and treated as corresponding to the $\mu^2 = 1 \text{ GeV}^2$ scale; then evolved to the reference point $\mu^2 = 4 \text{ GeV}^2$ of the global fits. 1-loop matching to $\overline{\text{MS}}$ still to be done on our data

A. Radyushkin 1710.08813, Zhang et al 1801.03023, Izubuchi et al 1801.03917

More on evolution



- LO evolution cannot be extended to very low scales.
- It is known that evolution stops below a certain scale (by observing our data we infer that this is the case for $z_3 \geq 6a$.)
- Adopt an evolution that leaves the PDF unchanged for length scales above $z_3 = 6a$ and use the leading perturbative evolution formula to evolve to smaller z_3 scales.

Numerical implementation

Following [C. Bouchard et.al Phys. Rev. D 96, no. 1, 014504 \(2017\)](#) , we compute a regular nucleon two point function

$$C_p(t) = \langle \mathcal{N}_p(t) \overline{\mathcal{N}}_p(0) \rangle ,$$

$$C_p^{\mathcal{O}^0(z)}(t) = \sum_{\tau} \langle \mathcal{N}_p(t) \mathcal{O}^0(z, \tau) \overline{\mathcal{N}}_p(0) \rangle$$

with $\mathcal{O}^0(z, t) = \overline{\psi}(0, t) \gamma^0 \tau_3 \hat{E}(0, z; A) \psi(z, t)$

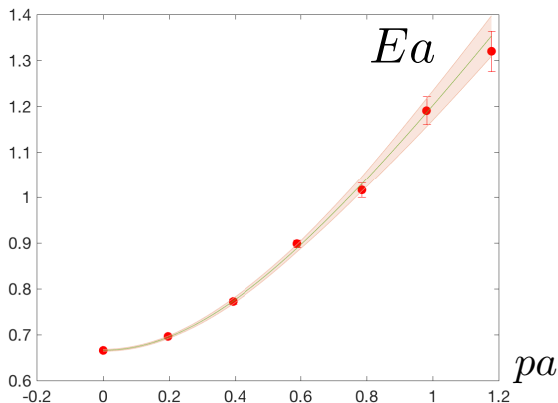
Proton momentum and displacement of the quark fields along the \hat{z} axis

$$\mathcal{M}_{\text{eff}}(z_3 p, z_3^2; t) = \frac{C_p^{\mathcal{O}^0(z)}(t+1)}{C_p(t+1)} - \frac{C_p^{\mathcal{O}^0(z)}(t)}{C_p(t)}$$

Extract the desired ME \mathcal{J} at large Euclidean time separation as

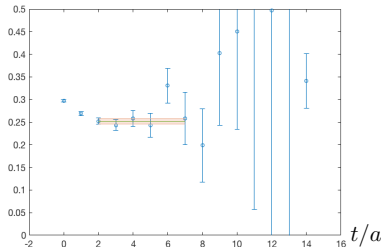
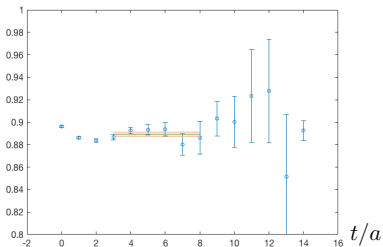
$$\frac{\mathcal{J}(z_3 p, z_3^2)}{2p^0} = \lim_{t \rightarrow \infty} \mathcal{M}_{\text{eff}}(z_3 p, z_3^2; t) , \text{ where } p^0 \text{ is the energy of the nucleon.}$$

Results for the nucleon dispersion relation



Energies and momenta are in lattice units. The solid line is the continuum dispersion relation (not a fit) while the errorband is an indication of the statistical error of the lattice nucleon energies

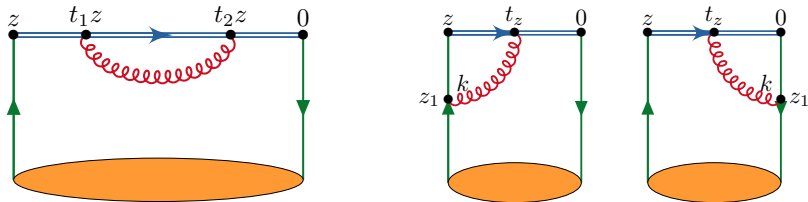
Results



Typical fits used to extract the reduced matrix element (here $p = 2\pi/L \cdot 2$ and $z = 4$ (LHS) and $p = 2\pi/L \cdot 3$ and $z = 8$ (RHS)). The average χ^2 per degree of freedom was $\mathcal{O}(1)$. All fits are performed with the full covariance matrix and the error bars are determined with the jackknife method.

Renormalization

- In a series of articles [Dotsenko Nucl.Phys. B169 \(1980\) 527](#), [Ishikawa et al. Phys. Rev. D 96, 094019 \(2017\)](#), [Chen et al. Nucl.Phys. B915 \(2017\)](#) and [A. V. Radyushkin Phys.Lett. B781 \(2018\) 433-442](#) the one loop renormalizability of $\mathcal{M}^\alpha(z, p, a)$ has been discussed
- by analyzing the pertinent diagrams one can see that there is a linear divergence from the link self-energy contribution and a logarithmic divergence associated to the anomalous dimension $2\gamma_{\text{end}}$ due to two end-points of the link.



Renormalization

- \mathcal{M} has been shown to renormalize multiplicatively as $\mathcal{M}_R(\nu, z^2, \mu) = Z_j^{-1} Z_{\bar{j}}^{-1} e^{-\delta m |z|} \mathcal{M}_B(\nu, z^2, a)$, where $\delta m = C_F \frac{\alpha_s}{2\pi} \frac{\pi}{a}$, is an effective mass counterterm removing power divergences in the Wilson line and $Z_j^{-1}, Z_{\bar{j}}^{-1}$ are renormalization constants (RCs) associated with the endpoints of the Wilson line independent of z, p .
- The entire renormalization is independent of the external momentum
- Forming the ratio, the RCs cancel and thus the reduced Ioffe time distribution has a great potential to reduce systematic effects related to renormalization. The UV divergences generated by the link-related and quark-self-energy diagrams cancel in the ratio.

Numerical implementation

- Renormalization of the ME?
- For $z_3 = 0$ $\mathcal{M}(z_3 p, z_3^2) \rightarrow$ the local iso-vector current, should be = 1 (but ...) lattice artifacts...
- Introduce an RC $Z_p = \frac{1}{\mathcal{J}(z_3 p, z_3^2)|_{z_3=0}}$
- Z_p has to be independent from p . But lattice artifacts or potential fitting systematics ...
- renormalize the ME for each momentum with its own $Z_p \rightarrow$ maximal statistical correlations to reduce statistical errors, and cancellation of lattice artifacts in the ratio

Numerical implementation

- in practise use the double ratio

$$\mathfrak{M}(\nu, z_3^2) = \lim_{t \rightarrow \infty} \frac{\mathcal{M}_{\text{eff}}(z_3 p, z_3^2; t)}{\mathcal{M}_{\text{eff}}(z_3 p, z_3^2; t)|_{z_3=0}} \times \frac{\mathcal{M}_{\text{eff}}(z_3 p, z_3^2; t)|_{p=0, z_3=0}}{\mathcal{M}_{\text{eff}}(z_3 p, z_3^2; t)|_{p=0}},$$

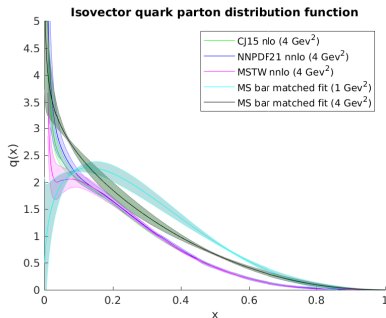
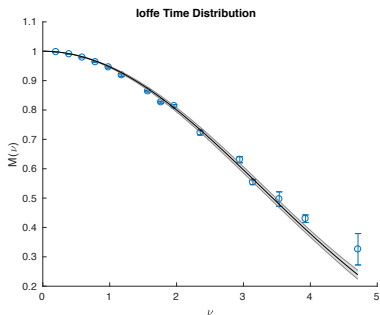
- infinite t limit is obtained with a fit to a constant for a suitable choice of a fitting range.

Matching to \overline{MS}

- In 1801.02427 it was shown by Radyushkin that at 1-loop evolution and matching to \overline{MS} can be done simultaneously.
- This establishes a direct relation between the Ioffe time distribution function (ITDF) and pseudo-ITDF.
- Scales are needed as such that we are in a regime dominated by perturbative effects

$$\begin{aligned} \mathcal{I}(\nu, \mu^2) = & \mathfrak{M}(\nu, z_3^2) + \frac{\alpha_s}{\pi} C_F \int_0^1 dw \mathfrak{M}(w\nu, z_3^2) \\ & \times \left\{ B(w) \ln \left[(1-w)z_3\mu \frac{e^{\gamma_E+1/2}}{2} \right] \right. \\ & \left. + [(w+1) \ln(1-w) - (1-w)]_+ \right\} \end{aligned}$$

Comparison to global fits after converting to the \overline{MS} scheme



Bayesian Reconstruction

$$P[q|\mathfrak{M}, I] = \frac{P[\mathfrak{M}|q, I]P[q|I]}{P[\mathfrak{M}|I]}.$$

- The likelihood probability $P[\mathfrak{M}|q, I]$ denotes how probable it is to find the data \mathfrak{M} if q were the correct PDF.
- Finding the most probable q by maximizing the likelihood is nothing but a χ^2 fit to the \mathfrak{M} data, which as we saw from the direct inversion is by itself ill-defined.
- The prior probability $P[q|I]$, which quantifies, how compatible our test function q is with respect to any prior information we have (e.g. appearance of non-analytic behavior of $q(x)$ at the boundaries of the x interval).
- $P[\mathfrak{M}|I]$, the so called evidence is a q independent normalization.

Bayesian Reconstruction

- For sampled data, due to the central limit theorem, the likelihood probability may be written as the quadratic distance functional $P[\mathfrak{M}|q, I] = \exp[-L]$ with $L = \frac{1}{2} \sum_{k,l} (\mathfrak{M}_k - \mathfrak{M}_k^q) C_{kl}^{-1} (\mathfrak{M}_l - \mathfrak{M}_l^q)$.
- \mathfrak{M}_k^q are the loffe-time data arising from inserting the test function q into the cosine Fourier trafo and C_{kl} denotes the covariance matrix of the N_m measurements of simulation data \mathfrak{M}_k^h .
- We then specify an appropriate prior probability $P[q|I] = \exp[\alpha S[I]]$.
- Prior information enters in two ways here. On the one hand we deploy a particular functional form of the regularization functional

$$S_{BR}[q, m] = \sum_n \Delta x_n \left(1 - \frac{q_n}{m_n} + \log\left(\frac{q_n}{m_n}\right) \right)$$

which may be obtained by requiring positive definiteness of the resulting q , smoothness of q .

Bayesian Reconstruction

- The functional S depends on the function m , the default model.
- By construction constitutes its unique extremum.
- In the Bayesian logic m is the correct result for q in the absence of any data.
- We select m by a best fit of the Ioffe-PDF data and we will vary it to get a handle on systematics.

Bayesian Reconstruction

- What happens in the case of non-guaranteed positive definiteness?
- We need to change the regulator!
- Often the quadratic regulator is used

$$S_{QDR}[q, m] = \sum_n \Delta x_n (q_n - m_n)^2$$

- It is a comparatively strong regulator and usually imprints the form of the default model significantly onto the end result.
- Trying to keep the influence of the default model to a minimum, we extend the BR prior to non-positive functions.

$$S_{BRg}[q, m] = \sum_n \Delta x_n \left(-\frac{|q_n - m_n|}{h_n} + \log\left(\frac{|q_n - m_n|}{h_n} - 1\right) \right)$$

keeping the advantageous properties of the original BR prior at the price of having to introduce another default model related function h .

Bayesian Reconstruction

- What happens in the case of non-guaranteed positive definiteness?
- We need to change the regulator!
- Often the quadratic regulator is used

$$S_{QDR}[q, m] = \sum_n \Delta x_n (q_n - m_n)^2$$

- It is a comparatively strong regulator and usually imprints the form of the default model significantly onto the end result.
- Trying to keep the influence of the default model to a minimum, we extend the BR prior to non-positive functions.

$$S_{BRg}[q, m] = \sum_n \Delta x_n \left(-\frac{|q_n - m_n|}{h_n} + \log\left(\frac{|q_n - m_n|}{h_n} - 1\right) \right)$$

keeping the advantageous properties of the original BR prior at the price of having to introduce another default model related function h .

Bayesian Reconstruction

- What happens in the case of non-guaranteed positive definiteness?
- We need to change the regulator!
- Often the quadratic regulator is used

$$S_{QDR}[q, m] = \sum_n \Delta x_n (q_n - m_n)^2$$

- It is a comparatively strong regulator and usually imprints the form of the default model significantly onto the end result.
- Trying to keep the influence of the default model to a minimum, we extend the BR prior to non-positive functions.

$$S_{BRg}[q, m] = \sum_n \Delta x_n \left(-\frac{|q_n - m_n|}{h_n} + \log\left(\frac{|q_n - m_n|}{h_n} - 1\right) \right)$$

keeping the advantageous properties of the original BR prior at the price of having to introduce another default model related function h .

Bayesian Reconstruction

- What happens in the case of non-guaranteed positive definiteness?
- We need to change the regulator!
- Often the quadratic regulator is used

$$S_{QDR}[q, m] = \sum_n \Delta x_n (q_n - m_n)^2$$

- It is a comparatively strong regulator and usually imprints the form of the default model significantly onto the end result.
- Trying to keep the influence of the default model to a minimum, we extend the BR prior to non-positive functions.

$$S_{BRg}[q, m] = \sum_n \Delta x_n \left(-\frac{|q_n - m_n|}{h_n} + \log\left(\frac{|q_n - m_n|}{h_n} - 1\right) \right)$$

keeping the advantageous properties of the original BR prior at the price of having to introduce another default model related function h .

Bayesian Reconstruction

- What happens in the case of non-guaranteed positive definiteness?
- We need to change the regulator!
- Often the quadratic regulator is used

$$S_{QDR}[q, m] = \sum_n \Delta x_n (q_n - m_n)^2$$

- It is a comparatively strong regulator and usually imprints the form of the default model significantly onto the end result.
- Trying to keep the influence of the default model to a minimum, we extend the BR prior to non-positive functions.

$$S_{BRg}[q, m] = \sum_n \Delta x_n \left(-\frac{|q_n - m_n|}{h_n} + \log\left(\frac{|q_n - m_n|}{h_n} - 1\right) \right)$$

keeping the advantageous properties of the original BR prior at the price of having to introduce another default model related function h .

Bayesian Reconstruction

- once L , S and m have been provided, the most probable PDF q , given simulation data and prior information is obtained by numerically finding the extremum of the posterior

$$\left. \frac{\delta P[q|\mathfrak{M}, I]}{\delta q} \right|_{q=q_{\text{Bayes}}} = 0.$$

- It has been proven that if the regulator is strictly concave, as is the case for all the regulators discussed above, there only exists a single unique extremum in the space of functions q on a discrete ν interval.
- With positive definiteness is imposed on the end result, the space of admissible solutions is significantly reduced. Regulators admitting also q functions with negative contributions have to distinguish between a multitude of oscillatory functions, which if integrated over, resemble a monotonous function to high precision. We will observe the emergence of ringing artefacts for the quadratic and generalized BR prior.

Bayesian Reconstruction

- The functional S depends on the function m , the default model.
- By construction constitutes its unique extremum.
- In the Bayesian logic m is the correct result for q in the absence of any data.
- We select m by a best fit of the Ioffe-PDF data and we will vary it to get a handle on systematics.
- In the definition of $P[q|I]$ we introduced a further parameter α , a so called hyperparameter
- Weighs the influence of simulation data and prior information. It has to be taken care of self-consistently.
- In the Maximum Entropy Method α is selected, such that the evidence has an extremum. In the BR method we deploy here, we marginalize the parameter α a priori, i.e. we integrate the posterior w.r.t the hyperparameter, assuming complete ignorance of its values $P[\alpha] = 1$.

Advanced PDF Reconstructions

- A versatile approach is Bayesian inference Y. Burnier and A. Rothkopf Phys.Rev.Lett. 111 (2013)
- It acknowledges the fact that the inverse problem is ill-defined and a unique answer may only be provided, once further information about the system has been made available.
- Formulated in terms of probabilities, one finds in the form of Bayes theorem that

$$P[q|\mathfrak{M}, I] = \frac{P[\mathfrak{M}|q, I]P[q|I]}{P[\mathfrak{M}|I]}.$$

It states that the so called **posterior probability** $P[q|\mathfrak{M}, I]$ for a test function q to be the correct x -space PDF, given our simulated loffe-time PDF \mathfrak{M} and additional prior information may be expressed in terms of three quantities.

Bayesian Reconstruction

$$P[q|\mathfrak{M}, I] = \frac{P[\mathfrak{M}|q, I]P[q|I]}{P[\mathfrak{M}|I]}.$$

- The likelihood probability $P[\mathfrak{M}|q, I]$ denotes how probable it is to find the data \mathfrak{M} if q were the correct PDF.
- Finding the most probable q by maximizing the likelihood is nothing but a χ^2 fit to the \mathfrak{M} data, which as we saw from the direct inversion is by itself ill-defined.
- The prior probability $P[q|I]$, which quantifies, how compatible our test function q is with respect to any prior information we have (e.g. appearance of non-analytic behavior of $q(x)$ at the boundaries of the x interval).
- $P[\mathfrak{M}|I]$, the so called evidence is a q independent normalization.

Bayesian Reconstruction

- For sampled data, due to the central limit theorem, the likelihood probability may be written as the quadratic distance functional $P[\mathfrak{M}|q, I] = \exp[-L]$ with $L = \frac{1}{2} \sum_{k,l} (\mathfrak{M}_k - \mathfrak{M}_k^q) C_{kl}^{-1} (\mathfrak{M}_l - \mathfrak{M}_l^q)$.
- \mathfrak{M}_k^q are the loffe-time data arising from inserting the test function q into the cosine Fourier trafo and C_{kl} denotes the covariance matrix of the N_m measurements of simulation data \mathfrak{M}_k^h .
- We then specify an appropriate prior probability $P[q|I] = \exp[\alpha S[I]]$.
- Prior information enters in two ways here. On the one hand we deploy a particular functional form of the regularization functional

$$S_{BR}[q, m] = \sum_n \Delta x_n \left(1 - \frac{q_n}{m_n} + \log\left(\frac{q_n}{m_n}\right) \right)$$

which may be obtained by requiring positive definiteness of the resulting q , smoothness of q .

Bayesian Reconstruction

- The functional S depends on the function m , the default model.
- By construction constitutes its unique extremum.
- In the Bayesian logic m is the correct result for q in the absence of any data.
- We select m by a best fit of the Ioffe-PDF data and we will vary it to get a handle on systematics.

Bayesian Reconstruction

- What happens in the case of non-guaranteed positive definiteness?
- We need to change the regulator!
- Often the quadratic regulator is used

$$S_{QDR}[q, m] = \sum_n \Delta x_n (q_n - m_n)^2$$

- It is a comparatively strong regulator and usually imprints the form of the default model significantly onto the end result.
- Trying to keep the influence of the default model to a minimum, we extend the BR prior to non-positive functions.

$$S_{BRg}[q, m] = \sum_n \Delta x_n \left(-\frac{|q_n - m_n|}{h_n} + \log\left(\frac{|q_n - m_n|}{h_n} - 1\right) \right)$$

keeping the advantageous properties of the original BR prior at the price of having to introduce another default model related function h .

Bayesian Reconstruction

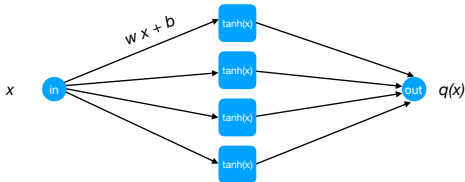
- once L , S and m have been provided, the most probable PDF q , given simulation data and prior information is obtained by numerically finding the extremum of the posterior

$$\left. \frac{\delta P[q|\mathfrak{M}, I]}{\delta q} \right|_{q=q_{\text{Bayes}}} = 0.$$

- It has been proven that if the regulator is strictly concave, as is the case for all the regulators discussed above, there only exists a single unique extremum in the space of functions q on a discrete ν interval.
- With positive definiteness is imposed on the end result, the space of admissible solutions is significantly reduced. Regulators admitting also q functions with negative contributions have to distinguish between a multitude of oscillatory functions, which if integrated over, resemble a monotonous function to high precision. We will observe the emergence of ringing artefacts for the quadratic and generalized BR prior.

Neural Network Reconstruction

- The ensemble average of data is obtained in two steps
 - ▶ Starting from random $[w, b]$, minimize χ^2 to find $[w, b]$.
 - ▶ Repeat 10 times to find 10 different Neural Nets (replicas).
- For each Neural Net, the minimizer is re-run for each jackknife sample to obtain a jackknife estimate $q(x)$ for each replica.
- Central value of $q(x)$ is the average over jackknife samples and replicas.
- Error by combining the fluctuations over the jackknife sample and replicas.



$$[\theta] = \{w, b\}$$

$$\min_{[\theta]} [\chi^2] \rightarrow [w, b]$$

$$\chi^2 = \sum_k \left(M(\nu_k) - \int_0^1 dx q_{[\theta]}(x) \cos(\nu_k x) \right) \sigma_k^2 \left(M(\nu_k) - \int_0^1 dx q_{[\theta]}(x) \cos(\nu_k x) \right)$$

Lattice QCD requirements

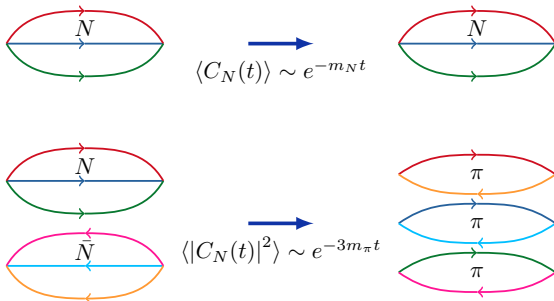
- Largest momentum on the lattice $aP_{max} = \pi/2 \propto \mathcal{O}(1)$
- $a = 0.1\text{fm} \rightarrow P_{max} = 10\Lambda$ where $\Lambda = 300 \text{ MeV}$
- $a = 0.05\text{fm} \rightarrow P_{max} = 20\Lambda$

Large momentum is required to suppress high twist effects (quasi-PDFs) and to provide a wide coverage of the loffe time ν

$P_{max} = 3 \text{ GeV}$ easily achievable with moderate values of the lattice spacing but still demanding due to statistical noise

$P_{max} = 6 \text{ GeV}$ exponentially harder requiring very fine values of the lattice spacing

Signal to Noise

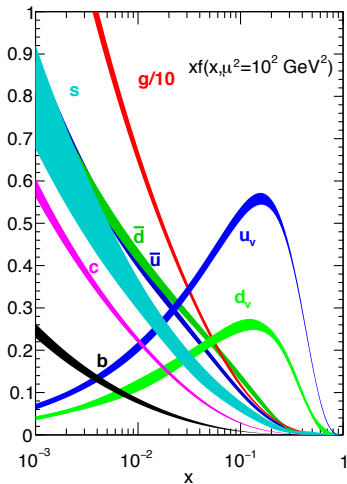
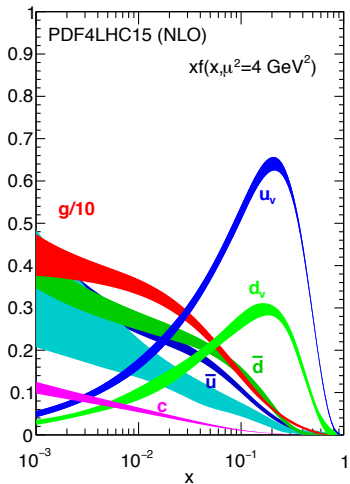


Statistical accuracy drops exponentially with increasing momentum P

$$\text{StN}(O) = \frac{\langle O \rangle}{\sqrt{\text{var}(O)}} \propto e^{-[E_N(P) - 3/2m_\pi]t}$$

G. Parisi (1984) P. Lepage (1989)

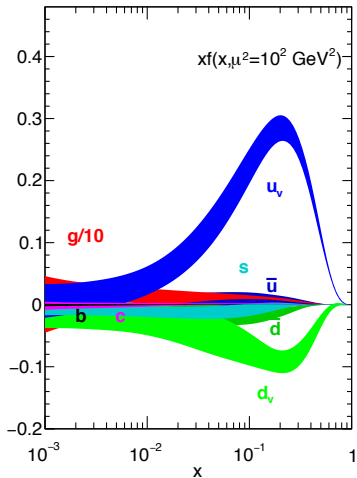
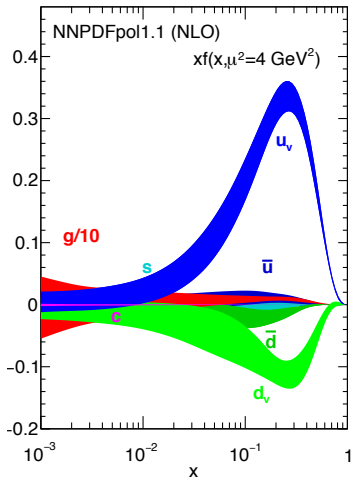
Determination of PDFs from Experiment



Global fits to experimental data [Parton distributions and lattice QCD calculations: a community white paper arXiv:1711.07916](#)

1711.07916

Determination of PDFs from Experiment



Global fits to experimental data [Parton distributions and lattice QCD calculations: a community white paper arXiv:1711.07916](#)

1711.07916

Backus-Gilbert Reconstruction

- The Backus-Gilbert (BG) method instead of imposing a smoothing condition on the resulting PDF $q(x)$ it imposes a minimization condition on the variance of the resulting function. G. Backus and F. Gilbert. Geophysical Journal of the Royal

Astronomical Society, 16:169205, (1968)

- Let us define a rescaled kernel and rescaled PDF $h(x)$

$$K_j(x) \equiv \cos(\nu_j x) p(x) \quad \text{and} \quad h(x) \equiv \frac{q_v(x)}{p(x)}$$

- where $p(x)$ corresponds to an appropriately chosen function that makes the problem easier to solve.
- We wish to incorporate into $p(x)$ most of the non-trivial structure of $q(x)$ apriorily, such that $h(x)$ is a slowly varying function of x and contains only the deviation of $q(x)$ from $p(x)$.

Backus-Gilbert Reconstruction

- Starting from the preconditioned expression with a rescaled PDF $h(x)$ that is only a slowly varying function of x our inverse problem becomes

$$d_j \equiv \mathfrak{M}_R(\nu_j) = \int_0^1 dx K_j(x) h(x).$$

- BG introduces a function $\Delta(x - \bar{x}) = \sum_j q_j(\bar{x}) K_j(x)$, where $q_j(\bar{x})$ are unknown functions to be determined.
- It then estimates the unknown function as a linear combination of the data

$$\hat{h}(\bar{x}) = \sum_j q_j(\bar{x}) d_j, \text{ or } \hat{q}_v(\bar{x}) = \sum_j q_j(\bar{x}) d_j p(\bar{x})$$

- If $\Delta(x - \bar{x})$ were to be a δ -function then $\hat{h}(\bar{x}) = h(\bar{x})$. If $\Delta(x - \bar{x})$ approximates a δ -function with a width σ , then the smaller σ is the better the approximation of $\hat{h}(x)$ to $h(x)$.

Backus-Gilbert Reconstruction

- In other words if $\hat{h}_\sigma(x)$ is the approximation resulting from $\Delta(x)$ with a width σ then $\lim_{\sigma \rightarrow 0} \hat{h}_\sigma(x) = h(x)$.
- With this in mind BG minimizes the width σ given by

$$\sigma = \int_0^1 dx (x - \bar{x})^2 \Delta(x - \bar{x})^2.$$

- Furthermore, if $\Delta(x)$ approximates a δ -function then one has to impose the constraint $\int_0^1 dx \Delta(x - \bar{x}) = 1$. Using a Lagrange multiplier λ one can minimize the width and impose the constraint by minimizing

$$\chi[q] = \int_0^1 dx (x - \bar{x})^2 \sum_{j,k} q_j(\bar{x}) K_j(x) K_k(x) q_k(\bar{x}) + \lambda \int_0^1 dx \sum_j K_j(x) q_j(\bar{x}).$$

- But let's see all this in practise ...